Discovery of Quinazolines as Histamine H_4 Receptor Inverse Agonists Using a Scaffold Hopping Approach

Rogier A. Smits,[†] Iwan J. P. de Esch,[†] Obbe P. Zuiderveld,[†] Joachim Broeker,[‡] Kamonchanok Sansuk,[†] Elena Guaita,[§] Gabriella Coruzzi,[§] Maristella Adami,[§] Eric Haaksma,[†,‡] and Rob Leurs*[,†]

Department of Pharmacochemistry, Faculty of Exact Sciences, Leiden/Amsterdam Center for Drug Research (LACDR), Division of Medicinal Chemistry, Vrije Universiteit Amsterdam, De Boelelaan 1083, 1081 HV Amsterdam, The Netherlands, Department of Medicinal Chemistry, Boehringer Ingelheim RCV GmbH & Co. KG, Dr. Boehringergasse 5-11, Vienna, Austria, and Department of Human Anatomy, Pharmacology and Forensic Medicine, Section of Pharmacology, University of Parma, Via Volturno 39, 43100 Parma, Italy

Received July 16, 2008

From a series of small fragments that was designed to probe the histamine H_4 receptor (H_4R), we previously described quinoxaline-containing fragments that were grown into high affinity H_4R ligands in a process that was guided by pharmacophore modeling. With a scaffold hopping exercise and using the same in silico models, we now report the identification and optimization of a series of quinazoline-containing H_4R compounds. This approach led to the discovery of 6-chloro-*N*-(furan-3-ylmethyl)2-(4-methylpiperazin-1-yl)quinazolin-4-amine (VUF10499, **54**) and 6-chloro-2-(4-methylpiperazin-1-yl)-*N*-(thiophen-2-ylmethyl)quinazolin-4-amine (VUF10497, **55**) as potent human H_4R inverse agonists (pK_i = 8.12 and 7.57, respectively). Interestingly, both compounds also possess considerable affinity for the human histamine H_1 receptor (H_1R) and therefore represent a novel class of dual action H_1R/H_4R ligands, a profile that potentially leads to added therapeutic benefit. Compounds from this novel series of quinazolines are antagonists at the rat H_4R and were found to possess anti-inflammatory properties in vivo in the rat.

Introduction

Histamine plays an important role in physiology and exerts its effects through the modulation of four known G-protein-coupled receptors (GPCRs[a]).[1] The H_1R receptor has long been known to be involved in allergic conditions. Its activation causes several responses such as vasoconstriction and increased vascular permeability leading to the characteristic symptoms in allergic rhinitis.[2] Several histamine H_1 receptor (H_1R) antagonists (e.g., cetirizine and loratidine) have reached blockbuster status because of their successful use in the treatment of allergic rhinitis.[3] The histamine H_2 receptor (H_2R) was discovered in 1972 and is well-known for its role in the regulation of the secretion of gastric acid.[4,5] Like the H_1R antagonists, H_2R antagonists (e.g., cimetidine and ranitidine) have also been widely prescribed, in this case for the treatment of gastric ulcers.[5] The H_3R was discovered in 1983, but major drug discovery efforts were only initiated after the identification of the H_3R gene in 1999.[6,7] The H_3R is mainly but not exclusively expressed in the central nervous system (CNS). Currently, H_3R ligands are studied in clinical trials for a variety of potential indications such as attention deficit hyperactivity disorder (ADHD) and narcolepsy.[8]

The histamine H_4 receptor (H_4R) is the latest addition to the family of G-protein-coupled histamine receptors. Although the receptor protein shows moderate homology to the H_3R (31% overall, 54% in the transmembrane region), it has a distinct pharmacological profile and a very different tissue distribution.[9−13]

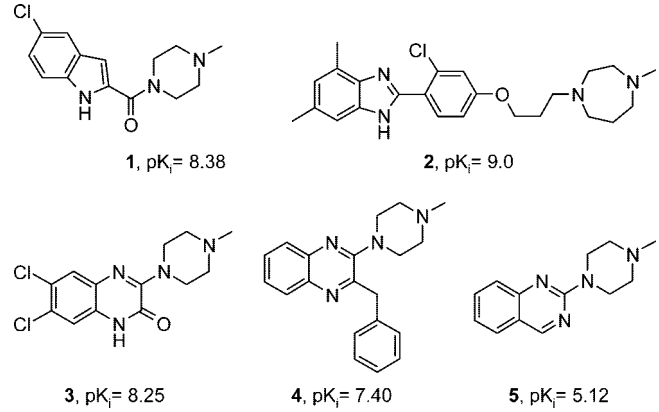

Figure 1. Several H_4 ligands and their reported potencies at the human H_4R.

The H_4R is mostly expressed on cells of the immune system and blood forming organs. Several lines of evidence suggest that the H_4R is a potential target for the treatment of asthma, pruritis, and rheumatoid arthritis.[14−17] It has also been suggested that in some cases (e.g., pruritis) additional clinically beneficial effects might be expected when H_1R and H_4R receptors are blocked simultaneously.[18]

Soon after the discovery of the H_4R receptor and the notion of its potential therapeutic value, combined high throughput screening and medicinal chemistry efforts identified the first non-imidazole antagonists, some with low nanomolar affinities (Figure 1).[19] The indole JNJ7777120 (**1**) is currently the prototypic H_4R antagonist used in most of the studies despite its very short half-life.[20] The more distinct benzimidazole (**2**) shows an improved H_4R affinity but has so far not been used in vivo.[21] Using a fragment-based approach, we recently reported the discovery of a series of quinoxalines as potent H_4R ligands (Figure 1). The 6,7-dichloro-substituted VUF10214 (**3**) is the most potent compound in this series.[22] Moreover, using

* To whom correspondence should be addressed. Phone: +31(0)205987600. Fax: +31(0)205987610. E-mail: leurs@few.vu.nl.
† Vrije Universiteit Amsterdam.
‡ Boehringer Ingelheim RCV GmbH & Co. KG.
§ University of Parma.

[a] Abbreviations: GPCRs, G-protein-coupled receptors; H_1R, histamine H_1 receptor; H_2R, histamine H_2 receptor; H_3R, histamine H_3 receptor; H_4R, histamine H_4 receptor; SAR, structure−activity relationship; CRE, cyclic AMP responsive element.

10.1021/jm800876b CCC: $40.75 © 2008 American Chemical Society
Published on Web 11/18/2008

Table 1. Quinazolines Substituted at the 4-Position with a Variety of Substituents

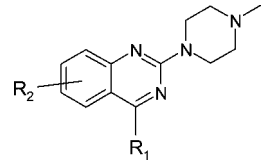

No.	R_1	R_2	$pK_i \pm SEM^a$	No.	R_1	R_2	$pK_i \pm SEM^a$
5	H	H	5.12±0.06	**39**		6-Cl	6.23±0.03
29	NH_2	H	5.67±0.07	**40**	$NHCH_3$	6-Cl	7.15±0.06
30	NH_2	6-Cl	6.98±0.08	**41**	$NHCH_3$	7-Cl	6.02±0.02
11	OH	6-Cl	4.82±0.15	**42**	$NHCH_3$	5-CH_3	6.16±0.03
31		H	5.55±0.03	**43**	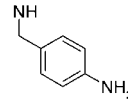	6-Cl	6.25±0.06
32	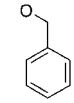	H	5.39±0.03	**44**	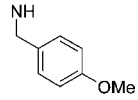	6-Cl	6.44±0.01
33		H	5.07±0.05	**45**	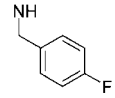	6-Cl	6.98±0.02
34	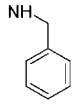	H	5.97±0.07	**46**	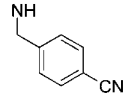	6-Cl	6.89±0.13
35	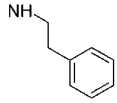	H	5.83±0.11	**47**	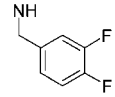	6-Cl	6.73±0.09
7	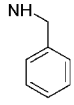	6-Cl	6.59±0.03	**48**	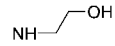	6-Cl	6.24±0.13
36	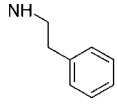	6-Cl	6.62±0.10	**49**	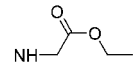	6-Cl	6.02±0.04
37		6-Cl	6.12±0.01	**50**		6-Cl	7.05±0.02
38		6-Cl	6.21±0.07	**51**		H	6.22±0.01

[a] Measured by displacement of [^{3}H]histamine binding using membranes of HEK cells transiently expressing the human H_4R. pK_i values are calculated from at least three independent measurements as the mean ± SEM.

an in-house developed pharmacophore model based on the flexible alignment of **1** and a rigid clozapine analogue,[23] we hypothesized the presence of a hydrophobic pocket in the H_4R active site that could be occupied by substituents on the 2-position of the quinoxaline heterocycle (Figure 2A). Indeed, several aromatic rings and aliphatic groups are tolerated on the quinoxaline scaffold, leading to, for example, VUF10148 (**4**), which possesses low, nanomolar H_4R affinity.[22]

In the previous fragment based approach we observed that besides the quinoxaline scaffold, a quinazoline heterocycle (Figure 1, compound **5**) also binds the H_4R with micromolar affinity.[22] Given the high structural similarity between the

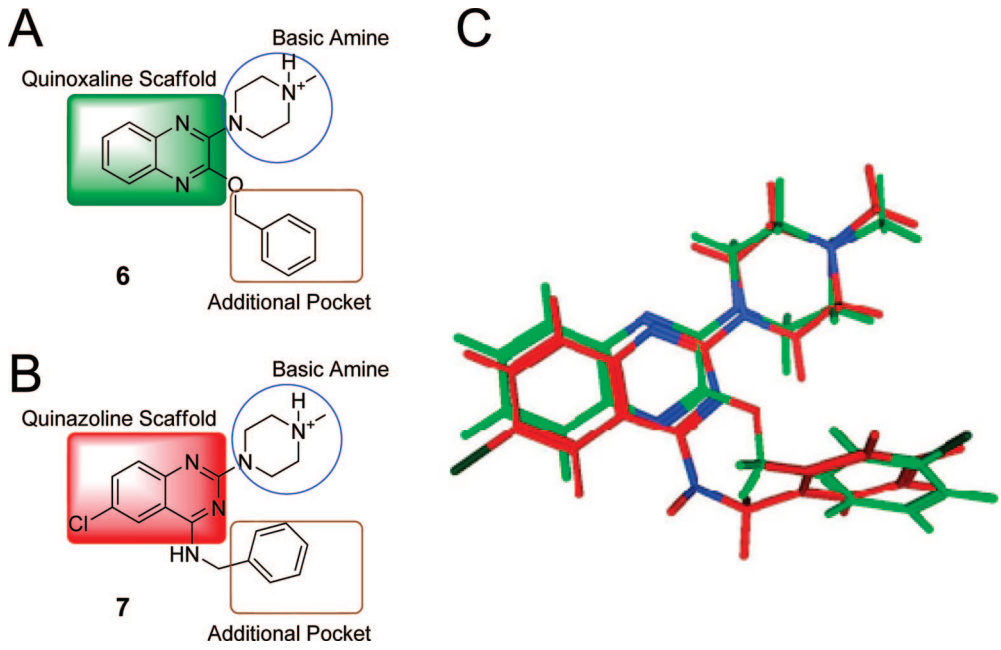

Figure 2. Scaffold hopping from quinoxalines to quinazolines as potential new ligands for the histamine H_4 receptor. Quinoxaline (A) (**6**, $pK_i = 6.57 \pm 0.05$) and quinazoline (B) (**7**) are proposed to have similar binding modes in this three pocket model. The flexible alignment of **6** and **7** (C) indicates that a similar low energy conformation can be adopted.

quinazoline and quinoxaline heterocycles, we assumed that both scaffolds might have overlapping binding modes in the H_4R binding site. The H_4R affinity of the quinoxaline series is determined by three important structural elements: a basic aminergic cyclic amine, a heterocyclic core with a small lipophilic substituent, and to a lesser extent the side chain on the 2-position (e.g., compound **6**, Figure 2A). On the basis of these structural elements, a scaffold hopping approach was attempted to obtain a new series of substituted quinazolines with high H_4R affinity.

Since in other series of H_4R antagonists the *N*-methylpiperazine moiety was found to be crucial for H_4R affinity, this basic amine was left unchanged in our initial series of quinazolines.[19,22−24] A chlorine atom was introduced on the 6-position (Figure 2B), since such a substituent is known to increase H_4R affinity in the quinoxaline series but also in chemically more distinct H_4R ligands such as indoles and benzimidazoles.[19,24] Substituents on the 4-position of the quinazoline heterocycle were expected to be tolerated to some extent or even to increase the H_4R affinity, as had been the case in the quinoxaline series.[22] Introducing a benzylamine group at the 4-position would give a ligand (**7**, Figure 2B) with a relatively flexible aromatic group that would be able to adopt a similar conformation as quinoxaline **6** (Figure 2C). In order to explore the SAR of such substituted quinazolines, we synthesized an initial series of compounds with diverse substituents ranging from aliphatics and aromatics to groups that are capable of forming hydrogen bonding interactions such as alcohols and esters (Tables 1 and 2).

Chemistry

Starting from 2-amino-5-chlorobenzoic acid (**8**), thioxoquinazoline **9** (Scheme 1) was prepared according to a procedure described in literature.[25] Intermediate **9** was subsequently alkylated with methyl iodide in aqueous sodium hydroxide to give intermediate **10**.[25] Heating of thioether **10** in neat *N*-methylpiperazine finally gave quinazolin-4-one **11**.

Commercially available anthranilic acids **8** and **12**−**16** were used to synthesize quinazolinediones **17**−**22** (Scheme 2) according to a modified procedure reported in literature.[26] 2,4-Dichloroquinazoline (**23**) was synthesized according to a procedure described in literature, whereas substituted dichloroquinazolines (**24**−**28**) were obtained by a modified procedure to give the desired products in very high purity.[27]

Disubstituted quinazolines **29**−**64** were prepared from their respective 2,4-dichlorosubstituted precursors (**23**−**28**, Scheme 2) and a set of commercially available primary amines using a one-pot procedure with microwave assisted heating. Intermediate 2-chloro substituted quinazoline **65** was synthesized by reacting **24** with methylamine. Subsequently, compound **65** was used for the preparation of compounds **66**−**81** by microwave assisted heating in the presence of diisopropylethylamine (DIPEA) while using *N*-methylpyrrolidone as a solvent.

The 2,4-dichloroquinazoline intermediates (**23**−**28**) could be selectively substituted at position 4 because of the lower reactivity of the carbon position 2. In a first step, we selectively introduced amines or alcohols at the 4-position at room temperature (rt). The reactivity of the alcohols was increased by deprotonation with sodium hydride (NaH) in dimethylformamide (DMF) in order to successfully react at room temperature. The selective introduction of the primary amines at the 4-position of **23**−**28** was effected at room temperature in the presence of DIPEA. These conversions were typically very high, and upon completion, excess *N*-methylpiperazine was subsequently introduced at the 2-position with microwave assisted heating. With this one-pot procedure, no workup of the 2-substituted quinazoline intermediate was required. In some cases the amines for substituting the 4-position needed to be used in excess (for compounds **29**, **30**, **38**, and **40**−**42**) because of the lack of reactivity of the 4-position at room temperature. In such cases, an intermediate workup to remove excess amine was required.

Results and Discussion

In the present study we focussed on applying a scaffold hopping approach and developing a new series of quinazolines as H_4R antagonists on the basis of the known SAR of related

Table 2. Quinazolines Substituted at the 4-Position with a Variety of Substituents

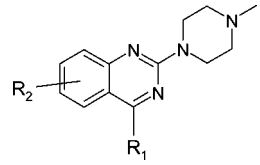

No.	R_1	R_2	$pK_i \pm$ SEM[a]	No.	R_1	R_2	$pK_i \pm$ SEM[a]
50		6-Cl	7.05±0.02	**58**	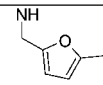	6-Cl	6.87±0.02
52		6-F	6.65±0.03	**59**	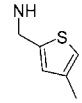	6-Cl	7.41±0.06
53		6-Cl, 8-CH_3	6.73±0.02	**60**		6-Cl	7.47±0.08
54		6-Cl	7.57±0.05	**61**	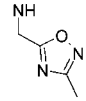	6-Cl	6.43±0.01
55		6-Cl	8.12±0.02	**62**		6-Cl	6.98±0.04
56		6-Cl	7.45±0.06	**63**		6-Cl	6.97±0.10
57	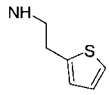	6-Cl	7.22±0.03	**64**	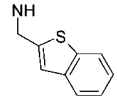	6-Cl	6.57±0.07

[a] Measured by displacement of [^{3}H]histamine binding using membranes of HEK cells transiently expressing the human H_4R. pK_i values are calculated from at least three independent measurements as the mean ± SEM.

Scheme 1[a]

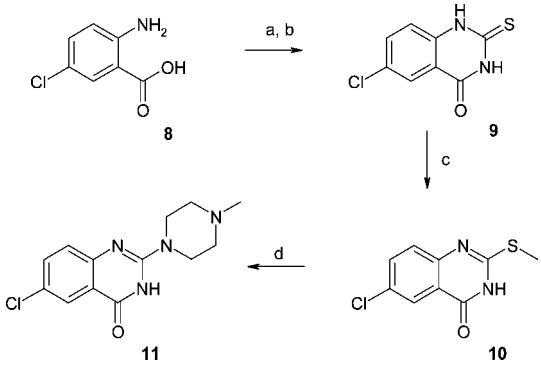

[a] Reagents and conditions: (a) $SOCl_2$, reflux; (b) NH_4SCN, acetone, rt; (c) CH_3I, aqueous NaOH, rt; (d) *N*-methylpiperazine, reflux.

quinoxalines.[22] Initially, we introduced various substituents at the 4-position of the quinazoline scaffold. Substitution of the 4-position (R_1 in Table 1) of quinazoline **5** with an amino function (**29**) leads to a 3-fold increase in affinity. Introducing an additional 6-chloro substituent (**30**) further boosts the activity up to a pK_i of 6.98 (Table 1), making compound **30** an interesting starting point for further optimization.

Surprisingly, the related quinazoline **11** has low affinity, indicating that the hydroxyl group of **11** is detrimental for H_4R affinity. In contrast, the introduction of a hydroxyl group in the quinoxaline series is very beneficial for H_4R affinity, leading to compounds with pK_i values in the range 8−9 (e.g., compound **3**, Figure 1).[22] Aromatic substitution of the hydroxyl group resulted in some gain in H_4R affinity, but the compounds remained only moderately active (**31** and **32**, Table 1). Phenyl substitution of the 4-amino group as in **33** was also not well tolerated, resulting in a 0.6 log unit loss in affinity. However, introducing an alkyl spacer between the amino group and the aromatic ring increased the affinity almost 10-fold again (**34**, Table 1). The introduction of a chlorine atom on the 6-position of these quinazolines leads to a further increase in H_4R affinity (compare **34** with **7** and **35** with **36**, Table 1). This beneficial effect is seen throughout this series and is in line with our hypothesis that a 6-chloro substituent on the heterocyclic quinazoline core would increase H_4R affinity. It is worth mentioning that quinazoline **7** was found to have a pK_i very similar to that of quinoxaline **6** (Figure 2), which was used as the original template for its design.

Aliphatic substitution of the amine function of **30** is generally not well tolerated and mostly leads to a reduction in H_4R affinity (Table 1, **37**−**39**). The only exception to this trend was the

Scheme 2[a]

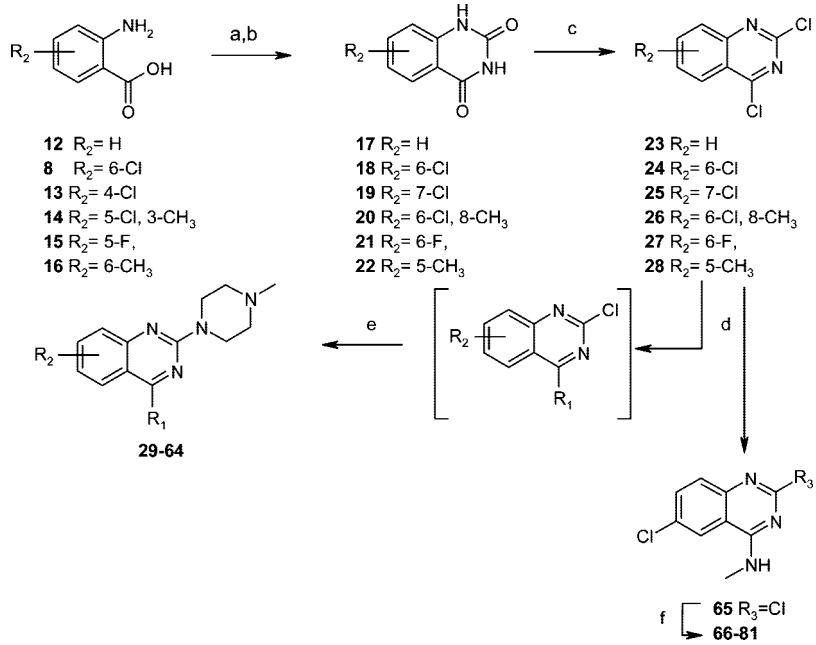

[a] Reagents and conditions: (a) urea, 160 °C; (b) 0.2 M NaOH, NaCl; (c) *N*,*N*-diethylaniline or DIPEA, $POCl_3$, reflux; (d) amine (R_1H), tetrahydrofuran or methanol or ethanol or ethyl acetate, DIPEA, rt; (e) ethyl acetate, *N*-methylpiperazine, 120 °C, 10 min; (f) amine (R_3H), *N*-methylpyrrolidone, DIPEA, microwave, 150 °C, 10 min.

methyl-substituted quinazoline **40**, which has a pK_i of 7.15. Since the H_4R affinity decreases when the size of the alkyl substituent increases, we speculate that in these compounds steric hindrance prevents the amino group from optimally interacting with the H_4R. We propose that the 4-amino group on the quinazoline scaffold acts as a hydrogen bond donor in binding to the H_4R. This proposal is supported by the observation that the sterically hindered aminophenylquinazoline **33** also shows moderate H_4R affinity. Increasing the length of the spacer between the amino group and a bulky amino substituent can regain some of the H_4R affinity that was lost as a result of steric shielding of the amino group (compare **33** with **34** and **35**). Replacement of the hydrogen atom on the methylamino group with an additional methyl group (**38**) results in the loss of the putative hydrogen bonding interaction, and the H_4R affinity drops approximately 8-fold (Table 1, compare **38** and **40**). Given the structural similarity of these 4-aminoquinazolines with the previously reported indolecarboxamide series (e.g., **1**, Figure 1), we suggest that the 4-aminoquinazolines make use of a similar hydrogen bonding interaction with the H_4R.[28] The basic amine in the *N*-methylpiperazine moiety of the quinazolines would then interact with aspartic acid residue Asp^{94} ($Asp^{3.32}$) in transmembrane helix 3 (TM3) through a salt bridge, and the hydrogen bond donor would interact with glutamic acid residue Glu^{182} ($Glu^{5.42}$) in TM5 through formation of a hydrogen bond.[28]

To further optimize **30**, a series of substituted benzylamines was synthesized (**43**−**47**, Table 1), but no major improvement was obtained. From this series one might expect opposing effects of electron-donating or -withdrawing substituents on H_4R affinity (Table 1). Compounds **48**−**51** were synthesized in an attempt to allow an additional hydrogen bond (e.g., with Glu^{182} ($Glu^{5.42}$)). Interestingly, the 2-furfurylaminoquinazoline **50** had a comparable affinity to **30**, indicating that a small aromatic ring was tolerated at this position. Also for **50** the 6-chloro atom is of substantial importance for the relatively high H_4R affinity (compare **50** with **51**, Table 1). Other substitution patterns did not lead to an increase in affinity (**52** and **53**, Table 2).

Following the discovery of **50**, some quinazolines with five-membered aromatic rings were synthesized to explore the SAR of such small aromatic heterocycles (**52**−**64**, Table 2). Moving the oxygen atom in the furan moiety of **50** from the 2- to the 3-position resulted in quinazoline **54** with 3-fold higher H_4R affinity. Replacement of the furan group of **50** by a thiophene moiety increased H_4R affinity 11-fold and resulted in the highly potent quinazoline analogue **55** with 7.5 nM affinity. Moving the sulfur atom of **55** from the 2- to the 3-position resulted in a loss of H_4R affinity (compare **55** and **56**). All other structural changes made to **50** and **55** such as extending the spacer length (**57**), introducing methyl substituents on the aromatic ring (**58**−**61**), introducing one or more additional heteroatoms (**61**−**63**), and increasing the heterocycle size (**64**) did not further improve the H_4R ligands.

The SAR of *N*-methylpiperazine replacements for H_4R activity has been reported for the indole and benzimidazole scaffolds.[19,22−24] From this work, we initially concluded that the *N*-methylpiperazine moiety is crucial for good H_4R activity. Nevertheless, some patent applications have described several H_4R ligands in which the *N*-methylpiperazine moiety has been successfully replaced with other cyclic amines.[29−32] We therefore investigated to what extent the quinazoline series would allow replacement of the *N*-methylpiperazine group. For coupling to the quinazoline scaffold we selected a set of cyclic amines (Table 3) with the following three structural elements: (1) at least two nitrogen atoms of which one could be directly attached to the aromatic heterocycle (proximal nitrogen atom), (2) a distal basic nitrogen atom potentially alkylated with a small aliphatic substituent, (3) an aliphatic ring system that would introduce a conformational restraint of the distal nitrogen atom. The 16 selected amines were coupled to 2,6-dichloro-*N*-methylquinazolin-4-amine (**65**) by a parallel synthesis method and evaluated for H_4R affinity in a [^{3}H]histamine displacement assay. Interestingly, compounds **73** and **74** displace [^{3}H]histamine binding to the H_4R with potency comparable to that of the parent compound **40** of this series. Further pharmacological evaluation ($n = 3$) resulted in a pK_i of 6.81 ± 0.02 ($n = 3$) for

Table 3. Affinity Screen of Quinazolines with *N*-Methylpiperazine Bioisosteres[a]

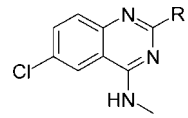

No.		$pK_i \pm SEM$[a]	No.	R_1	$pK_i \pm SEM$[a]
40	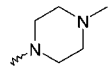	7.15±0.06			
66	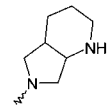	<6	**74**	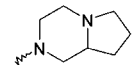	6.85±0.02
67	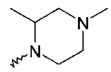	<6	**75**	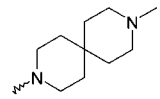	<6
68	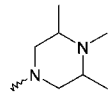	<6	**76**		<6
69	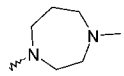	<6	**77**	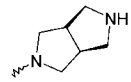	<6
70	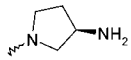	<6	**78**	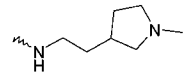	<6
71	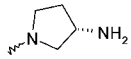	<6	**79**	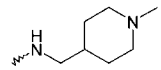	<6
72	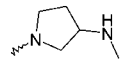	<6	**80**	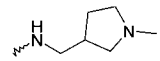	<6
73	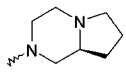	6.81±0.02	**81**	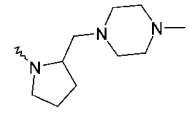	<6

[a] Measured by displacement of [^{3}H]histamine binding using membranes of HEK cells transiently expressing the human H_4R. pK_i values are calculated from at least three independent measurements as the mean ± SEM. Substitutions with more than a 10-fold loss ($pK_i < 6$) in affinity compared to **40** are considered unsuccessful. Compounds **73** and **74** were found to have H_4R affinities very similar to that of parent compound **40**.

compound **73** and a pK_i of 6.85 ± 0.02 ($n = 3$) for compound **74** compared to a pK_i of 7.15 ± 0.06 ($n = 3$) for the parent compound **40**. Because no difference in affinity was found between the *S*-enantiomer **73** and its racemic mixture **74**, we conclude that there is no significant affinity difference between the *R*- and *S*-enantiomers of diazabicyclo[4.3.0]nonane substituted quinazolines. Interestingly, several of the amines in Table 3 that have been reported to be tolerated on other H_4R scaffolds (e.g., **66**, **69**, **72**, and **77**) are very detrimental to H_4R affinity on the quinazoline scaffold.[31−33] From the tested series of cyclic amines, we conclude that the *N*-methylpiperazine moiety in our 4-aminoquinazoline scaffold can be replaced with its bioisostere diazabicyclo[4.3.0]nonane without significant loss of affinity.

For the most potent examples from the optimized quinazoline scaffold, we selected compounds **54** and **55** for further evaluation. As explained in the Introduction, our studies were guided by our three-pocket pharmacophore model (Figure 2) on the basis of the flexible alignment of **1** and a close analogue (VUF6884, **82**, H_4R $pK_i = 7.55 \pm 0.10$) of the antipsychotic drug clozapine (Figure 3A).[23] The van der Waals interaction surface of this flexible alignment model was generated to map the surface of the binding site of the H_4R. The two pockets in which the *N*-methylpiperazine and aromatic heterocycles bind the H_4R are clearly visible as well as the proposed third hydrophobic pocket (Figure 3A). After flexible alignment of quinazolines **54** and **55** with compounds **1** and **82** it was found that the quinazolines can adopt a low energy conformation in which the furan (**54**) and thiophene (**55**) can occupy the proposed hydrophobic third pocket while occupying the other two pockets with the *N*-methylpiperazine and quinazoline moieties (Figure 3B).

On the basis of the same model, we previously developed benzylquinoxaline **4**, which appears to combine good H_4R affinity with a reasonable H_1R affinity (H_1R $pK_i = 6.0$).[22] Clozapine analogue **82** also possessed high H_1R affinity ($pK_i = 8.11$),[23] prompting us to speculate that filling the third putative

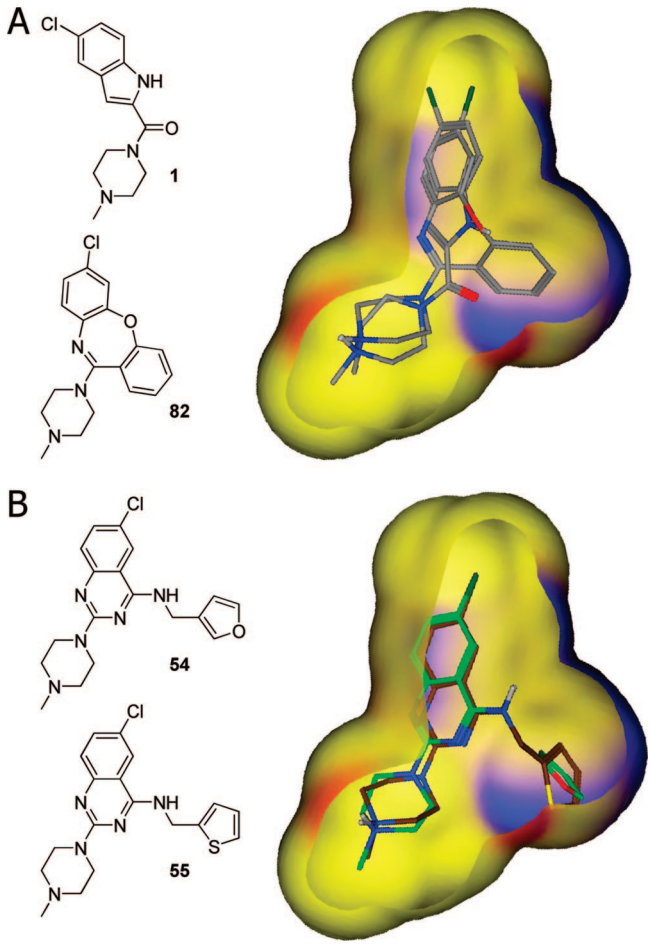

Figure 3. Model of the H_4R binding site. The hydrophobic (van der Waals) surface is depicted in yellow, mild polar surface in blue, and potential sites for hydrogen bonding interaction in red. (A) The model based on the alignment of **1** and **82** reveals three pockets, with the proposed third hydrophobic pocket on the right-hand side. (B) Quinazolines **54** (green) and **55** (brown) fit the binding site and occupy the third pocket with their furan and thiophene moieties, respectively.

Table 4. Affinity and Functional Profile of Compounds **54** and **55** at the Humane Histamine H_1 and H_4 Receptors

54		**55**	
receptor	$pK_i \pm$ SEM[a]	receptor	$pK_i \pm$ SEM[a]
human H_4	7.57 ± 0.05	human H_4	8.12 ± 0.02
human H_1	7.01 ± 0.10	human H_1	7.70 ± 0.10

[a] Measured by displacement of radioligand binding using previously described methods from literature.[35,22] pK_i values are calculated from at least three independent measurements as the mean ± SEM.

pocket (Figure 3), e.g., with aromatic groups, greatly increases H_4R affinity of quinazoline **30** but might also lead to substantial H_1R affinity. This hypothesis is supported by the observation that quinoxalinone **3** (Figure 1) has very high H_4R affinity but does not bind the H_1R.[22] Quinoxalinone **3** fits in two pockets of the pharmacophore model but does not occupy the third pocket with an aromatic substituent, thereby explaining its lack of H_1R affinity. The pharmacology of compounds **54** and **55** was therefore studied at the human histamine H_1R subtype (Table 4). Interestingly, both **54** and **55** were found to possess considerable affinity for the H_1R and to be almost equipotent at both the H_1R and H_4R.

With a pK_i of 8.12, quinazoline **55** is significantly more effective (9-fold) in displacing [^{3}H]histamine binding from the H_4R compared to the standard imidazole-containing inverse agonist thioperamide ($pK_i = 7.28 \pm 0.02$, Figure 4A). Quinazoline **54** ($pK_i = 7.57$) has an affinity close to that of thioperamide. Next, we examined the functional activities of the new compounds on the human H_4R. In an H_4R-driven CRE-β-galactosidase reporter gene assay, histamine shows full agonistic behavior ($\alpha = 1$) (Figure 4B), whereas thioperamide behaves as an invere agonist ($\alpha = -1$). Compound **54** displays pronounced inverse agonistic behavior ($\alpha = -1.49$), whereas **55** ($\alpha = -1.06$) shows inverse agonism comparable to thioperamide. At the rat H_4R, **54** and **55** have respective pK_i values of 7.61 ± 0.21 and 7.80 ± 0.02 and behave as neutral antagonists (data not shown). Compound **55** was thereafter selected to study the anti-inflammatory effect on this new series of H_4R ligands in the carrageenan induced paw edema model for inflammation.[34] After 2 h, compound **55** caused a significant inhibition of carrageenan-induced edema at both 10 and 30 mg/kg when compared to vehicle (Figure 5). This effect was still significant 4 h after administration.

In conclusion, this work describes the design and synthesis of a novel series of quinazolines as inverse agonists for the histamine H_4 receptor. These quinazolines are closely related to a series of quinoxalines reported by our group in a previous disclosure.[22] The quinoxalines provided the basis for the molecular design and subsequent scaffold hopping that led to this novel series of quinazoline compounds. After pharmacological evaluation, they were found to have high affinity up to the single-digit nanomolar range while showing inverse agonistic behavior at the human H_4R. In addition, we were able to successfully replace the most commonly encountered structural element of H_4R ligands, the *N*-methylpiperazine group, with a suitable diazabicyclo[4.3.0]nonane bioisostere while retaining H_4R affinity. Since the most potent compounds possessed considerable affinity for the histamine H_1 receptor subtype, the quinazoline scaffold may be a good starting point for the development of a new class of dual action H_1R/H_4R antihistamines. The three-pocket pharmacophore model apparently allows for the design of dual action ligands. Such compounds might be used to treat the acute symptoms of inflammatory conditions. For example, allergic rhinitis could be treated by blockade of the H_1R, similar to the mode of action of the H_1R antiallergic antihistamines (e.g., loratidine and cetirizine), while simultaneously targeting the H_4R to modulate the underlying disease mechanism by blocking the influx of proinflammatory cells.[18] Such dual action H_1R/H_4R ligands may prove to be superior to the selective H_1R antihistamines or selective H_4R antihistamines that are exclusively targeted at one of either receptor.[18]

Experimental Section

General Remarks. Chemicals and reagents were obtained from commercial suppliers and were used without further purification. The amines for compounds **67**, **68**, **70**, **71**, and **74**−**81** were generously donated by Boehringer Ingelheim RCV GmbH & Co. KG, Vienna, Austria. Yields given are isolated yields unless mentioned otherwise. Flash column chromatography was typically carried out on an Argonaut Flashmaster II flash chromatography system, using prepacked Silicycle Flash Si II columns with the UV detector operating at 254 nm. All melting points are uncorrected and were measured on an Optimelt automated melting point system from Stanford research systems. All ^{1}H NMR and ^{13}C NMR spectra were measured on a Brüker 200 or Brüker 250. Analytical HPLC−MS analyses were conducted using a Shimadzu LC-8A preparative liquid chromatograph pump system with a Shimadzu SPD-10AV UV−vis detector with the MS detection performed with a Shimadzu LCMS-2010 liquid chromatograph mass spectrometer. The buffer mentioned under conditions I and II is a 0.4% (w/v)

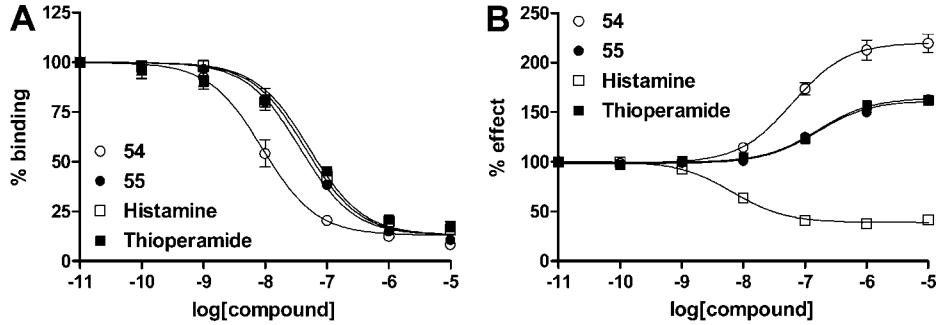

Figure 4. (A) Compounds **54** and **55** bind to the hH_4R with high affinity as determined by [^{3}H]histamine displacement. (B) Quinazolines **54** ($\alpha = -1.49$) and **55** ($\alpha = -1.06$) show inverse agonistic behavior in a functional assay (CRE-galactosidase reporter gene) performed in parallel with H_4R agonist histamine and H_4R inverse agonist thioperamide. The α values for histamine and thioperamide have been arbitrarily set at 1 and -1, respectively. Corresponding pIC_{50} values for **54** and **55** are 6.84 ± 0.12 and 7.16 ± 0.04, respectively ($n = 3$).

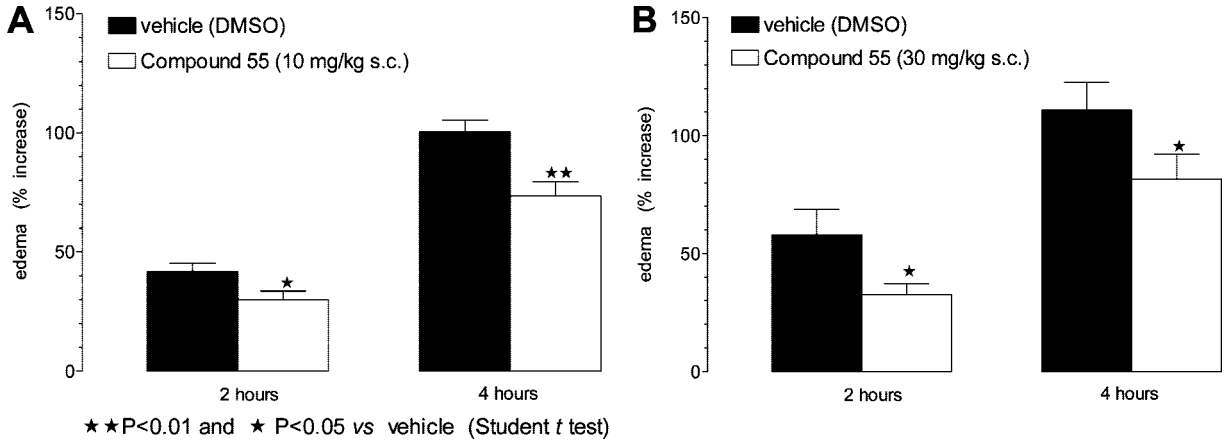

Figure 5. Anti-inflammatory effects of compound **55** on paw edema induced by subplantar injection of carrageenan (1% in CMC) in rats. Data are expressed as the mean ± SEM, $n = 6$ rats per group. Comparisons between multiple groups were made by using one-way analysis of variance (ANOVA), followed by Dunnett's test: (∗) $P < 0.05$ and (∗∗) $P < 0.01$ compared with vehicle-treated animals (Student t test for grouped data).

NH_4CO_3 solution in water, adjusted to pH 8.0 with NH_4OH. The analyses were performed using the following two conditions. Condition I: an Xbridge (C18) 5 μm column (100 mm × 4.6 mm) with solvent A (90% MeCN−10%) and solvent B (90% water−10% buffer), flow rate of 2.0 mL/min, start 5% A, linear gradient to 90% A in 10 min, then 10 min at 90% A, then 10 min at 5% A, total run time of 30 min. Condition II: Xbridge (C18) 5 μm column (100 mm × 4.6 mm) with solvent A (MeCN with 0.1% formic acid) and solvent B (water with 0.1% formic acid), flow rate of 2.0 mL/min, start 5% A, linear gradient to 90% A in 10 min, then 5 min at 90% A, then 5 min at 5% A, total run time of 20 min. Compound purities under both conditions were calculated as the percentage peak area of the analyzed compound by UV detection at 254 nm. Analytical HPLC−MS analyses for condition III were carried out on Agilent 1100 series HPLC−MS system including an Agilent G1315B DAD. Condition III: XBridge (C18) 3.5 μm column (2.1 mm × 50 mm) with solvent A (a 5 mM solution of NH_4HCO_3 in water set to pH 9.0 using 19 mM NH_3) and solvent B (100% ACN), MS detection with an Agilent G1956B LC/MSD SL using a multimode ion source, flow rate of 1.2 mL/min, start 95% A, linear gradient to 5% A in 1.25 min, then 0.75 min at 5% A, followed by 1.0 min 95% A, 5% B, total run time of 3 min. Preparative HPLC−MS separations were carried out on an Agilent 1100 series preparative HPLC−MS system including a G1968D active splitter, G1315B DAD, and a G1946D LC/MSD using an ESI ion source. Elution was done over a Waters X-Terra MS C18 5 μm column (19 mm × 100 mm) with the solvent A (a 10 mM solution of NH_4HCO_3 in water set to pH 9.5 using 38 mM NH_3) and solvent B (100% ACN), flow rate of 30 mL/min, gradient of 30% B → 75% B, start 70% A, 30% B, 1.3 min isocratic elution, 6.0 min to 25% A, 75% B followed by 0.7 min to 95% A, 5% B, then 1.0 min at 5% A and 95% B, followed by 1.8 min 75% A, 30% B, total run time of 10.8 min.

In Vitro Pharmacology. Radioligand Displacement Studies at the Human H_1 and H_4 Receptors. The pK_i values at the H_1R and H_4R were determined as described before.[35,22]

H_4R CRE-β-galactosidase Assay. Five million HEK 293T cells (in a suspension of 500 000 cell/mL) were transfected with a mixture containing 2.5 μg of pCRE-gal, 5 μg of receptor plasmid, and 35 μg of a 25 kDa linear polyethyleneimine and transferred into a transparent 96-well plate. Twenty-four hours after transfection, cells were stimulated with ligands in the presence of 1 μM forskolin for 6 h. Thereafter, the medium was discarded, the cells were lysed in 100 μL of assay buffer (100 mM sodium phosphate buffer at pH 8.0, 4 mM ONPG, 0.5% Triton X-100, 2 mM $MgSO_4$, 0.1 mM $MnCl_2$, 40 mM β-mercaptoethanol) and incubated at room temperature for up to 4 h. The β-galactosidase activity was determined at 420 nm with a Powerwave X340 plate reader (Bio-Tek Instruments, Inc.).[36] The data were analyzed using Prism 4.0 (Graphpad Software Inc.).

Flexible Alignment Models. The flexible alignment models were created with Molecular Operating Environment 2006.08 (MOE) from Chemical Computing Group (Montreal, Canada). The compounds in Figure 2 were aligned with the flexible alignment module of MOE using default parameters and similarity term "partial charge" added with a weight factor (WF) of 1. The alignment with lowest alignment score S and average strain energy score U ($S = 227.7783$, $U = 98.9762$, F (similarity score) $= 128.8201$) was selected and refined further using the "refine existing alignment" option with an energy cutoff of 7.0 kcal/mol. Compounds **1** and **82** were aligned with the following similarity terms and associated weight factors: H-bond donor (WF = 3), aromaticity (WF = 3),

polar hydrogens (WF = 1), and volume (WF = 3). The lowest alignment score *S* was then selected and refined further using the "refine existing alignment" option with an energy cutoff of 7.0 kcal/mol. The van der Waals surface map for Figure 3A was generated with a distance of 4.5 Å. The final alignment of **1** and **82** was then fixed, and compounds **54** and **55** were both separately aligned with **1** and **82** using the flexible alignment module with the similarity terms described for the alignment of **1** and **82**. The final alignments were selected on the basis of the best fit: for **54**, lowest objective function score *S* (*S* = 73.2264, *U* = 17.9301, *F* = 55.3363); for **55**, third lowest objective function score *S* (*S* = 71.3573, *U* = 19.0853, *F* = 52.1195).

In Vivo Pharmacology. Carrageenan-Induced Edema Model. Male Wistar rats (180−200 g; Harlan-Italy, Milan, Italy) were housed under controlled standard conditions (23 °C, 12 h light/dark cycle, and 65% humidity). Food and water were provided ad libitum. The experiments received the approval of the local Animal Ethics Committee of the University of Parma, Italy. Inflammation was induced in fasted rats by subplantar injection of carrageenan (0.1 mL of 1% suspension in carboxymethycellulose) into the left hind paw. As previously described, carrageenan-induced edema was measured with a plethysmometer (Basile, Comerio, Italy) immediately prior to the injection of carrageenan and thereafter at 2, 4, and 6 h.[34] Edema was expressed for each animal as percent increase in paw volume after carrageenan injection relative to the preinjection value, considered as 100. Equivalent volumes (0.1 mL per 100 g) of compound **55** or vehicle were administered subcutaneously (sc) in separate groups of rats immediately prior to carrageenan injection. Before use, a solution of the histamine H_4 receptor ligand in dimethyl sulfoxide was freshly prepared. Data are expressed as the mean ± SEM. $P < 0.05$ was considered statistically significant. Prism GraphPad 3.0 (GraphPad Software Inc., San Diego, CA) was used to process data.

Synthetic Methods. General Method A. The following method is representative for the synthesis of 2,4-disubstituted quinazolines **29**, **33**, **35**−**39**, and **43**−**64**.

***N*-Benzyl-2-(4-methylpiperazin-1-yl)quinazolin-4-amine (34).** 2,4-Dichloroquinazoline (171 mg, 0.86 mmol) was added to a microwave tube containing EtOAc (3.0 mL) and DIPEA (0.32 mL, mmol). Benzylamine (94 μL, 0.86 mmol) was added, and the resulting mixture was stirred at room temperature until TLC indicated complete conversion of the starting material to the monosubsituted quinazoline. *N*-Methylpiperazine (1.0 mL) was added, and the reaction mixture was heated at 120 °C for 10 min under microwave irradiation. The obtained suspension was then diluted with EtOAc (50 mL) and washed with water and brine. Drying of the organic phase with Na_2SO_4 and evaporation of the solvent gave the crude product that was purified over SiO_2 (90% EtOAc, 5% Et_3N, 5% MeOH) to yield 398 mg (79%) mg of the title compound as a beige solid. Mp 132.4−134.6 °C; ^{1}H NMR ($CDCl_3$) δ 7.50−7.24 (m, 7H), 7.07−7.00 (m, 1H), 5.80 (m, 1H), 4.78 (d, J = 5.4 Hz, 2H), 3.91 (t, J = 5.0 Hz, 4H), 2.45 (t, J = 5.0 Hz, 4H), 2.32 (s, 3H); ^{13}C NMR ($CDCl_3$) δ (ppm) 159.48, 158.62, 151.92, 138.63, 132.45, 128.53, 127.74, 127.33, 125.65, 120.88, 120.56, 110.19, 54.99, 46.10, 45.03, 43.71; MS (ESI) *m*/*z* 334 $(M + H)^+$.

General Method B. The following method is representative for the synthesis of 2,4-disubstituted quinazoline ether **32**.

2-(4-Methylpiperazin-1-yl)-4-phenoxyquinazoline (31). 2,4-Dichloroquinazoline (300 mg, 1.52), phenol (170 mg, 1.81 mmol), and NaH (55 mg of a 60% dispersion in mineral oil, 2.28 mmol) in DMF (5.0 mL) were stirred at room temperature. After 2 h the reaction mixture was diluted with EtOAc and water. The aqueous phase was extracted with ethyl acetate, and the combined organic layers were washed with H_2O and brine. After the mixture was dried over Na_2SO_4 and after evaporation of the solvent, the obtained product was transferred to a microwave tube containing *N*-methylpiperazine (2.0 mL). The mixture was heated at 140 °C for 5 min under microwave irradiation. The product was diluted with ethyl acetate and washed with H_2O and brine. After the mixture was dried over Na_2SO_4 and subsequent evaporation of the solvent, the residue was purified over SiO_2 (EtOAc 90%, Et_3N 5%, MeOH 5%), yielding 20 mg (4%) of a light-yellow solid. Mp 102.2−103.1 °C; ^{1}H NMR ($CDCl_3$) δ (ppm) 8.09 (d, J = 8.2 Hz, 1H), 7.67−7.38 (m, 4H), 7.27−7.16 (m, 4H), 3.72 (t, J = 5.0 Hz, 4H), 2.38 (t, J = 5.0 Hz, 4H), 2.29 (s, 3H); ^{13}C NMR ($CDCl_3$) δ (ppm) 166.82, 157.81, 154.01, 152.48, 133.93, 129.08, 125.15, 124.94, 123.64, 122.01, 121.83, 111.01, 54.64, 45.80, 43.34; MS (ESI) *m*/*z* 321 $(M + H)^+$.

General Method C. The following method is representative for the synthesis of 2,4 diamino substituted quinazolines **66**−**81**.

6-Chloro-4-methylamino(4-methyl-1,4-diazepan-1-yl)quinazoline (69). A microwave tube was charged with 2,6-dichloro-*N*-methylquinazolin-4-amine (100 mg, 0.44 mmol), diisopropylethylamine (113 μL, 0.66 mmol), *N*-methylpyrrolidinone (200 μL), and *N*-methylhomopiperazine (75 μL, 0.60 mmol). The mixture was then heated at 150 °C for 10 min, and the obtained solution was transferred to a LC−MS vial using a small amount of *N*-methylpyrrolidinone. The reaction mixture was directly purified with preparative LC−MS and freeze-dried to yield the title compound as a white solid. Compounds **66**, **70**−**72**, and **77** were synthesized from *tert*-butyl octahydro-1*H*-pyrrolo[3,4-*b*]pyridine-1-carboxylate, (*R*)-*tert*-butyl pyrrolidin-3-ylcarbamate, (*S*)-*tert*-butyl pyrrolidin-3-ylcarbamate, *tert*-butyl methyl(pyrrolidin-3-yl)carbamate and (3a*R*,6a*S*)-*tert*-butyl hexahydropyrrolo[3,4*c*]pyrrole-2(1*H*)-carboxylate, respectively. After purification by LC−MS the Boc-protected intermediates were deprotected by stirring in 2 M dioxane/HCl until LC−MS indicated complete conversion. Removal of the solvent yielded the desired amines as hydrochloride salts.

General Method D. The following method is representative for the synthesis of chloroquinazoline-2,4(1H, 3*H*)-diones **19**−**22**.

6-Chloroquinazoline-2,4(1*H*,3*H*)-dione (18). A flask containing urea (15.0 g, 0.25 mol) and 2-amino-5-chlorobenzoic acid (4.25 g, 24.8 mmol) was heated at 140 °C. After being stirred for 6 h, the reaction mixture was cooled to 100 °C and an equal volume of water was added. The obtained suspension was left to stir for 10 min, after which it was cooled to room temperature. The precipitate was filtered off and was dissolved in an aqueous 0.2 M NaOH solution (∼100 mL). The solution was then heated at 100 °C for 5 min, causing a white precipitate to form. After being stirred at room temperature overnight, the solution was acidified to pH 7 with concentrated HCl and a white solid was filtered off. The obtained solid was washed with water, triturated with hot EtOH (100 mL), and cooled to room temperature. After filtration of the suspension and drying of the product in vacuo, the title compound was obtained as 2.81 g (14.3 mmol, 58%) of a white solid. ^{1}H NMR (DMSO-d_6) (ppm) δ 11.37 (app bs, 2H), 7.80 (d, J = 2.5 Hz, 1H), 7.68 (dd, J = 8.7 Hz, J = 2.5 Hz, 1H), 7.18 (d, J = 8.7 Hz, 1H).

General Method E. The following method is representative for the synthesis of 2,4-dichloroquinazolines **25**−**28**.

2,4,6-Trichloroquinazoline (24). 6-Chloro-2,4-dihydroxyquinazoline (1.41 g, 7.17 mmol), *N*,*N*-diethylaniline (2.3 mL), and $POCl_3$ (5.0 mL) were heated at reflux. After 3 h the mixture was cautiously poured over crushed ice. The obtained suspension was stirred. The solids were extracted with DCM, and the combined organic phases were washed with brine. Drying over Na_2SO_4 and evaporation of the solvent yielded 1.52 g (6.51, 91%) of a yellow solid. The solid was dissolved in DCM and filtered over a pad of silica using DCM as eluent to yield the title compound as a white solid. Mp 129.1−130.8 °C; ^{1}H NMR ($CDCl_3$) (ppm) δ 8.23−8.22 (m, 1H), 7.97−7.87 (m, 2H).

6-Chloro-2-(4-methylpiperazin-1-yl)quinazolin-4(3*H*)-one (11). 6-Chloro-2-(methylthio)quinazolin-4(3*H*)-one (**10**) (1.0 g, 4.41 mmol) was added to *N*-methylpiperazine (15.2 mL), and the resulting mixture was heated at reflux. After 4 h the mixture was diluted with water and washed with EtOAc. The aqueous phase was then acidified with concentrated HCl to pH 7, causing the desired product to crystallize from the solution. The solid was filtered off and recrystallized from EtOH to yield 567 mg (2.03 mmol, 46%) of white crystals. ^{1}H NMR (DMSO-d_6) δ (ppm) 7.82 (d, J = 2.5 Hz, 1H), 7.60 (dd, J = 2.5 Hz, J = 8.8 Hz, 1H), 7.30

(d, $J = 8.8$ Hz, 1H), 3.62 (t, $J = 4.9$ Hz, 4H), 2.37 (t, $J = 4.9$ Hz, 4H), 2.20 (s, 3H); MS (ESI) *m/z* 279 $(M + H)^+$.

2,4,7-Trichloroquinazoline (25). 7-Chloroquinazolin-2,4(1*H*,3*H*)-dione (1.03 g, 5.21 mmol), DIPEA (1.91 mL, 10.95 mmol), and $POCl_3$ (5.0 mL) were heated at reflux. After 4 h the hot mixture was carefully poured onto crushed ice, causing a precipitate to form after vigorous stirring. The formed suspension was extracted with CH_2Cl_2, and the organic phases were combined. After the mixture was washed with brine and dried over Na_2SO_4, the solvent was removed and the title compound was obtained as a yellow solid that was used in the next step without further purification. Yield: 1.124 g (96%). ^{1}H NMR (DMSO-d_6) δ (ppm) 8.17 (d, $J = 9.0$ Hz, 1H), 7.96 (d, $J = 2.0$ Hz), 7.66 (d, $J = 2.0$ Hz, $J = 9.0$ Hz, 1H).

6-Chloro-2-(4-methylpiperazin-1-yl)quinazolin-4-amine (30). 2,4,6-Trichloroquinazoline (300 mg, 1.28 mmol) was added to a saturated solution of ammonia in MeOH (5.0 mL) and stirred at room temperature. After 16 h the mixture was diluted with EtOAc (50 mL) and washed with water and brine. After the mixture was dried over Na_2SO_4, the organic phase was concentrated (about 3 mL) and transferred to a microwave tube containing *N*-methylpiperazine (1.0 mL). The mixture was heated at 140 °C for 5 min using microwave irradiation. The formed suspension was then diluted with EtOAc and washed with water and brine. Subsequent drying over Na_2SO_4 and evaporation of the solvent yielded an orange solid that was purified over SiO_2 (EtOAc 90%, Et_3N 5%, MeOH 5%). The title compound was obtained as 276 mg (78%) of a light-yellow solid. Mp 176.0−178.5 °C; ^{1}H NMR ($CDCl_3$) δ (ppm) 7.46−7.34, (m, 3H), 5.30 (s, 2H), 3.86 (t, $J = 5.1$ Hz, 4H), 2.44 (t, $J = 5.1$ Hz, 4H), 2.31 (s, 3H); ^{13}C NMR ($CDCl_3$) δ (ppm) 160.59, 158.81, 151.24, 133.51, 127.37, 125.64, 120.96, 110.10, 54.98, 46.11, 43.59; MS (ESI) *m/z* 278 $(M + H)^+$.

6-Chloro-*N*-methyl-2-(4-methylpiperazin-1-yl)quinazolin-4-amine (40). 2,4,6-Trichloroquinazoline (300 mg, 1.28 mmol) was dissolved in THF (5.0 mL) after which a solution of methylamine in water (0.12 mL of 40% w/w in water) was added to the solution. After 2 h the formed suspension was diluted with EtOAc (50 mL) and washed with water and brine. The organic phase was dried over Na_2SO_4 and concentrated (approximately 3 mL), after which it was transferred to a microwave tube containing *N*-methylpiperazine (1.0 mL) and EtOAc (3.0 mL). The mixture was heated at 140 °C for 5 min with microwave irradiation. The product was then diluted with EtOAc and washed with water and brine. Subsequent drying over Na_2SO_4 and evaporation of the solvent yielded a dark-yellow oil that was purified over SiO_2 (EtOAc 90%, Et_3N 5%, MeOH 5%). The title compound was obtained as a light-yellow solid. Yield: 308 mg (1.06 mmol, 82%). Mp 173.2−175.7 °C; ^{1}H NMR ($CDCl_3$): δ (ppm) 7.42−7.24 (m, 3H), 5.42 (s, 1H), 3.92 (t, $J = 4.8$ Hz, 4H), 3.10 (d, $J = 4.8$ Hz, 3H), 2.46 (t, $J = 4.8$ Hz, 4H), 2.32 (d, $J = 1.0$ Hz, 3H); ^{13}C NMR ($CDCl_3$) δ (ppm) 159.47, 158.84, 150.49, 132.73, 127.27, 125.42, 119.99, 110.98, 55.03, 46.12, 43.61, 27.96; MS (ESI) *m/z* 292 $(M + H)^+$.

2,6-Dichloro-*N*-methylquinazolin-4-amine (65). To a suspension of 2,4,6-trichloroquinazoline (4.70 g, 20.1 mmol) in EtOH (150 mL) was added methylamine (1.91 mL of 40% w/w in water). The mixture was then stirred at room temperature for 40 min, after which the solution was concentrated to a volume of about 30 mL. The reaction mixture was then diluted with water (200 mL) and extracted with EtOAc. The combined organic layers were washed with brine and dried over Na_2SO_4. Evaporation of the solvent yielded 3.90 g (17.1, 85%) of a white-yellow solid that was used in the next step without further purification. Mp 198.2−205.0 °C. ^{1}H NMR (DMSO-d_6) (ppm) δ 8.88 (br s, 1H), 8.35 (d, $J = 2.3$ Hz, 1H), 7.81 (dd, $J = 2.3$ Hz, $J = 8.9$ Hz, 1H), 7.63 (d, $J = 8.9$ Hz, 1H), 2.99 (s, 3H).

(*S*)-6-Chloro-2-(hexahydropyrrolo[1,2-*a*]pyrazin-2(1*H*)-yl))-*N*-methylquinazolin-4-amine (73). 2,6-Dichloro-*N*-methylquinazolin-4-amine (**65**) (150 mg, 0.67 mmol), DIPEA (0.74 mmol, 0.13 mL), and (*S*)-diazabicyclo[4.3.0]nonane (0.74 mmol, 93 mg) were added to a microwave tube with EtOAc (2.0 mL). After the mixture was heated for 10 min at 130 °C, it was diluted with EtOAc and washed with saturated $NaHCO_3$ and brine. The organic layer was dried over Na_2SO_4 and evapoated to dryness. The solid residue was purified over SiO_2 (EtOAc 90%, Et_3N 5%, MeOH 5%) to yield 186 mg (87%) of the title compound. ^{1}H NMR ($CDCl_3$) δ (ppm) 7.44−7.35 (m, 3H), 5.45 (d, $J = 4.2$ Hz, 1H), 5.06−4.89 (m, 2H), 3.18−3.02 (m, 6H), 2.74−2.65 (m, 1H), 2.29−2.11 (m, 2 H), 2.02−1.74 (m, 4H), 1.56−1.50 (m, 1H); ^{13}C NMR ($CDCl_3$) δ (ppm) 159.46, 158.76, 150.50, 132.73, 127.14, 125.41, 120.07, 110.97, 62.53, 53.43, 52.00, 48.25, 43.10, 27.99, 27.14, 21.06; MS (ESI) *m/z* 318 $(M + H)^+$.

Acknowledgment. Thanks goes to Debora Granemann for synthetic assistance. The authors also greatly appreciate the technical assistance of Frans de Kanter.

Supporting Information Available: Purity data for compounds **5**, **7**, **11**, and **29**-**64** as determined by LC−MS; experimental details for compounds **7**, **19**−**22**, **26**−**29**, **32**, **33**, **35**−**39**, and **41**−**64**. This material is available free of charge via the Internet at http://pubs.acs.org.

References

(1) de Esch, I. J. P.; Thurmond, R. L. J. A.; Jongejan, A.; Leurs, R. The histamine H_4 receptor as a new therapeutic target for inflammation. *Trends Pharmacol. Sci.* **2005**, *26*, 462–469.
(2) Hill, S., J. Distribution, properties and functional characteristics of three classes of histamine receptor. *Pharm. Rev.* **1990**, *42*, 45–83.
(3) Klabunde, T.; Hessler, G. Drug design strategies for targeting G-protein-coupled receptors. *ChemBioChem* **2002**, *3*, 928–944.
(4) Black, J. W.; Garbarg, M.; Durant, G., J.; Ganellin, C., R.; Parsons, M. E. Definition and antagonism of histamine H_2-receptors. *Nature* **1972**, *236*, 385–390.
(5) Berardi, R., R.; Tankanow, R., M.; Nostrant, T., T. Comparison of famotidine with cimetidine and ranitidine. *Clin. Pharm.* **1988**, *7*, 271–284.
(6) Arrang, J., M.; Garbarg, M.; Schwartz, J., C. Auto-inhibition of brain histamine release mediated by a novel class (H_3) of histamine receptor. *Nature* **1987**, *302*, 832–837.
(7) Lovenberg, T., W.; Roland, B., L.; Wilson, S., J.; Jiang, X.; Pyati, J.; Huvar, A.; Jackson, M. R.; Erlander, M. E. Cloning and functional expression of the human histamine H_3 receptor. *Mol. Pharmacol.* **1999**, *55*, 1101–1107.
(8) Wijtmans, M.; Leurs, R.; de Esch, I. Histamine H_3 receptor ligands break ground in a remarkable plethora of therapeutic areas. *Expert Opin. Invest. Drugs* **2007**, *16*, 967–985.
(9) Liu, C.; Ma, X.-J.; Jiang, X.; Wilson, S. J.; Hofstra, C. L.; Blevitt, K.; Li, X.; Chai, W.; Carruthers, N.; Lovenberg, T. W. Cloning and pharmacological characterization of a fourth histamine receptor (H_4) expressed in bone marrow. *Mol. Pharmacol.* **2001**, *59*, 420–426.
(10) Morse, K. l.; Behan, J.; Laz, T. M., Jr.; Greenfender, S. A.; Anthes, J. C.; Umland, S.; Wan, Y.; Hipkin, R. W.; Gonsiorek, W.; Shin, N.; Gustafson, E. L.; Qiao, X.; Wang, S.; Hedrick, J. A.; Green, J.; Bayne, M.; Monsma, F. J., Jr. Cloning and characterization of a novel human histamine receptor. *J. Pharmacol. Exp. Ther.* **2001**, *296*, 1058–1066.
(11) Nguyen, T.; Shapiro, D. A.; George, S. R.; Setola, V.; Lee., D. K.; Cheng, R.; Rauser, L.; Lee, S. P.; Lynch, K. R.; Roth, B. L.; O'Dowd, B. F. Discovery of a novel member of the histamine receptor family. *Mol. Pharmacol.* **2001**, *59*, 427–433.
(12) Oda, T.; Morikawa, N.; Saito, Y.; Masuho, Y.; Matsumoto, S. Molecular cloning and characterization of a novel type of histamine receptor preferentially expressed in leukocytes. *J. Biol. Chem.* **2000**, *275*, 36781–36786.
(13) Zhu, Y.; Michalovich, D.; Wu, H.-L.; Tan, K. B.; Dytko, G. M.; Mannan, I. J.; Boyce, R.; Alston, J.; Tierney, L. A.; Li, X.; Herrity, N. C.; Vawter, L.; Sarau, H. M.; Ames, R. S.; Davenport, C. M.; Hieble, J. P.; Wilson, S.; Bergsma, D. J.; Fitzgerald, L. R. Cloning, expression and pharmacological characterization of a novel human histamine receptor. *Mol. Pharmacol.* **2001**, *59*, 434–444.
(14) Dunford, P. J.; O'Donnel, N.; Riley, J.; Williams, K., N.; Karlsson, L.; Thurmond, R., L. The histamine H_4 receptor mediates allergic airway inflammation by regulating the activation of $CD4^+$ T cells. *J. Immunol.* **2006**, *176*, 7062–7070.
(15) Dunford, P. J.; Williams, K. N.; Desai, P. J.; Karlsson, L.; McQueen, D.; Thurmond, R. L. Histamine H_4 receptor antagonists are superior to traditional antihistamines in the attenuation of experimental pruritis. *J. Allergy Clin. Immunol.* **2007**, *119*, 176–183.
(16) Ohki, E.; Suzuki, M.; Aoe, T.; Ikawa, Y.; Negishi, E.; Ueno, K. Expression of histamine H_4 receptor in synovial cells from rheumatoid arthritis patients. *Biol. Pharm. Bull.* **2007**, 2217–2220.

(17) Rossbach, K.; Wendorff, S.; Sander, K.; Stark, H.; Gutzmer, R.; Werfel, T.; Kietzmann, M.; Bäumer, W. Histamine H_4 antagonism reduces hapten-induced scratching behavior but not inflammation *Exp. Dermatol.*, in press.
(18) Daugherty, B., L. Histamine H_4 antagonism: a therapy for chronic allergy. *Br. J. Pharmacol.* **2004**, *142*, 5–7.
(19) Jablonowski, J. A.; Grice, C. A.; Dvorak, C. A.; Venable, J. D.; Kwok, A. K.; Ly, K. S.; Wei, J.; Baker, S. M.; Desai, P. J.; Jiang, W.; Wilson, S. J.; Thurmond, R. L.; Karlsson, L.; Edwards, J. P.; Lovenberg, T. W.; Carruthers, N. I. The first potent and selective non-imidazole human histamine H_4 receptor antagonists. *J. Med. Chem.* **2003**, *19*, 3957–3960.
(20) Thurmond, R. L.; Desai, P. J.; Dunford, P. J.; Fung-Leung, W. P.; Hofstra, C. L.; Jiang, W.; Nguyen, S.; Riley, J. P.; Sun, S.; Williams, K. N.; Edwards, J. P.; Karlsson, L. A potent and selective histamine H_4 receptor antagonist with anti-inflammatory properties. *J. Pharmacol. Exp. Ther.* **2004**, *309*, 404–413.
(21) Lee-Dutra, A.; Arienti, K. L.; Buzard, D. J.; Hack, D.; Khatuya, H.; Desai, P.; Nguyen, S.; Thurmond, R. L.; Karlsson, L.; Edwards, J. P.; Breitenbucher, J. G. Identification of 2-arylbenzimidazoles as potent human histamine H_4 receptor ligands. *Bioorg. Med. Chem. Lett.* **2006**, *16*, 6043–6048.
(22) Smits, R. A.; Lim, H. D.; Hanzer, A.; Zuiderveld, O. P.; Guaita, E.; Adami, M.; Coruzzi, G.; Leurs, R.; de Esch, I. J. P. Fragment based design of new H_4 receptor-ligands with anti-inflammatory properties in vivo. *J. Med. Chem.* **2008**, *51*, 2457–2467.
(23) Smits, R. A.; Lim, H. D.; Stegink, B.; Bakker, R. A.; de Esch, I. J. P.; Leurs, R. Characterization of the histamine H_4 receptor binding site. Part I. Synthesis and pharmacological evaluation of dibenzodiazepine derivatives. *J. Med. Chem.* **2005**, *49*, 4512–4516.
(24) Terzioglu, N.; van Rijn, R. M.; Bakker, R. A.; de Esch, I. J. P.; Leurs, R. Synthesis and structure−activity relationships of indole- and benzimidazole piperazines as histamine H_4 receptor antagonists. *Bioorg. Med. Chem. Lett.* **2004**, *14*, 5251–5256.
(25) Somers, F.; Ouedraogo, R.; Antoine, M.; de Tullio, P.; Becker, B.; Fontaine, J.; Damas, J.; Dupont, L.; Rigo, B.; Delarge, J.; Lebrun, P.; Pirotte, B. Original 2-alkylamino-6-hologenoquinazolin-4(3*H*)-ones and K_{ATP} channel activity. *J. Med. Chem.* **2001**, *44*, 2575–2585.
(26) Lee, A. H. F.; Kool, E. T. Novel benzopyrimidines as widened analogues of DNA bases. *J. Org. Chem.* **2005**, *70*, 132–140.
(27) Curd, F. H. S.; Landquist, J. K.; Rose, F. L. *J. Chem. Soc.* **1947**, 775.
(28) Jongejan, A.; Lim, H. D.; Smits, R. A.; de Esch, I. J.; Haaksma, E.; Leurs, R. Delineation of agonist binding to the human histamine H_4 receptor using mutational analysis, homology modeling and ab initio calculations. *J. Chem. Inf. Model.* **2008**, *48*, 1455–1463.
(29) Sato, H.; Fukushima, K.; Shimazaki, M.; Urbahns, K.; Sakai, K.; Ganter, F.; Bacon, K. 2-Aminopyrimidine Derivatives. Patent WO2005054239, June 16, 2005.
(30) Bell, A. S.; Lane, C. A. L.; Mowbray, C. E.; Selby, M. D.; Swain, N. A.; Williams, D. H. Pyrimidine Derivatives. Patent WO2007072163, June 28, 2007.
(31) Reid, A.; Wilson, F.; Dyke, H.; Price, S.; Cramp, S. Enantiomers of Amino Pyrimidine Compounds for the Treatment of Inflammatory Disorders. Patent WO2007090853, August 16, 2007.
(32) Lane, C. A. L.; Price, D. A. Octahydropyrrolo[3,4-*c*]pyrrole Derivatives. Patent US20060111416, May 25, 2006.
(33) Edwards, J. P.; Savall, B. M.; Shah, C. R. Indoles and Benzimidazoles As Modulators of the Histamine H_4 Receptor. Patent WO2007117401, October 18, 2007.
(34) Coruzzi, G.; Adami, M.; Guaita, E.; de Esch, I. J. P.; Leurs, R. Antiinflammatory and antinociceptive effects of the selective histamine H_4-receptor antagonists JNJ7777120 and VUF6002 in a rat model of carrageenan-induced inflammation. *Eur. J. Pharmacol.* **2007**, *563*, 240–244.
(35) Bakker, R. A.; Weiner, D., M.; ter Laak, T.; Beuming, T.; Zuiderveld, O., P.; Edelbroek, M.; Hacksell, U.; Timmerman, H.; Brann, M., R.; Leurs, R. 8*R*-Lisuride is a potent stereospecific histamine H1-receptor partial agonist. *Mol. Pharmacol.* **2004**, *65*, 538–549.
(36) Lim, H. D.; van Rijn, R. M.; Ling, P.; Bakker, R. A.; Thurmond, R. L.; Leurs, R. Evaluation of histamine H_1-, H_2-, and H_3-receptor ligands at the human histamine H_4 receptor: identification of 4-methylhistamine as the first potent and selective histamine H_4 receptor agonist. *J. Pharmacol. Exp. Ther.* **2005**, *314*, 1310–1321.

JM800876B